Interactions of cationic trimeric, gemini and monomeric surfactants with trianionic curcumin in aqueous solution

ARTICLE *in* SOFT MATTER · MARCH 2014

Impact Factor: 4.03 · DOI: 10.1039/c4sm00086b · Source: PubMed

6 AUTHORS, INCLUDING:

Meina Wang
Lund University
6 PUBLICATIONS **19** CITATIONS
SEE PROFILE

Yongqiang Tang
Chinese Academy of Sciences
9 PUBLICATIONS **29** CITATIONS
SEE PROFILE

Yaxun Fan
Chinese Academy of Sciences
14 PUBLICATIONS **96** CITATIONS
SEE PROFILE

Han Yuchun
Chinese Academy of Sciences
47 PUBLICATIONS **603** CITATIONS
SEE PROFILE

Soft Matter

PAPER

View Article Online
View Journal | View Issue

Cite this: *Soft Matter*, 2014, **10**, 3432

Interactions of cationic trimeric, gemini and monomeric surfactants with trianionic curcumin in aqueous solution†

Meina Wang, Chunxian Wu, Yongqiang Tang, Yaxun Fan, Yuchun Han and Yilin Wang*

Interactions of trianionic curcumin (Cur^{3-}) with a series of cationic surfactants, monomeric surfactant dodecyl trimethylammonium bromide (DTAB), dimeric surfactant hexamethylene-1,6-bis(dodecyldimethylammonium bromide) (12–6–12) and trimeric surfactant tri(dodecyldimethylammonioacetoxy)diethyltriamine trichloride (DTAD), have been investigated in aqueous solution of pH 13.0. Surface tension and spectral measurements indicate that the cationic surfactants display a similar surfactant concentration dependent interaction process with Cur^{3-}, involving three interaction stages. At first the three cationic surfactants electrostatically bind on Cur^{3-} to form the surfactant–Cur^{3-} complex. Then the bound and unbound cationic surfactants with Cur^{3-} aggregate into surfactant–Cur^{3-} mixed micelles through hydrophobic interactions above the critical micelle concentration of the surfactants (CMC_C) in the presence of Cur^{3-}. Finally excess unbound surfactants self-assemble into micelles like those without Cur^{3-}. For all the three surfactants, the addition of Cur^{3-} only decreases the critical micelle concentration of 12–6–12 but does not affect the critical micelle concentration of DTAB and DTAD. As the oligomeric degree of surfactants increases, the intermolecular interaction of the cationic surfactants with Cur^{3-} increases and the surfactant amount needed for Cur^{3-} encapsulation decreases. Compared with 12–6–12, either the weaker interaction of DTAB with Cur^{3-} or stronger interaction of DTAD with Cur^{3-} limits the stability or solubility of Cur^{3-} in surfactant micelles. Therefore, gemini surfactant 12–6–12 is the best choice to effectively suppress Cur^{3-} degradation at very low concentrations. Isothermal titration microcalorimetry, surface tension and ^{1}H NMR results reveal that 12–6–12 and Cur^{3-} form a $(12–6–12)_2$–Cur^{3-} complex and start to form micelles at extremely decreased concentrations, where either 12–6–12 or Cur^{3-} works as a bridge linkage and the resultant structure exhibits the characteristics of oligomeric surfactants.

Received 14th January 2014
Accepted 11th February 2014

DOI: 10.1039/c4sm00086b

www.rsc.org/softmatter

Introduction

Curcumin is a naturally occurring yellow-orange pigment extracted from the rhizome of turmeric and contains two ferulic acid residues covalently linked through a methylene bridge. Recent reports have proved that curcumin in aqueous solution exists predominantly in the enol form.[1,2] Studies over the past few decades have shown that curcumin possesses effective antioxidant,[3] anticancer,[4,5] anti-inflammatory,[6] anti-Alzheimer's disease[7] and other desirable medicinal functions.[8]

However, a major problem in the application of curcumin is its poor aqueous solubility at acidic and neutral pH values (~20 μg mL^{-1}) because of the hydrophobic nature. This problem can be solved by increasing the pH of aqueous solution where pH sensitive curcumin will dissociate into anionic species. But this dissociation will result in a rapid degradation of curcumin by alkaline hydrolysis.[9,10] Thus, various encapsulation approaches have been designed to improve the water solubility and stability of curcumin. Loading of curcumin into surfactant micelles is one of the promising convenient means. Some studies have shown that micelle solution is highly effective in enhancing aqueous solubility of curcumin at acid and neutral pHs up to ~740 μg mL^{-1}.[11,12] Under basic conditions, hydrophobic microdomains of micelles can segregate curcumin from the alkaline aqueous phase and diminish or reduce the degradation as long as curcumin diffuses through the interface of micelles. The diminishing or reducing extent depends on the structure of surfactants in micelles. English *et al.*[13] and Kee *et al.*[14] revealed that micelles formed by cationic monomeric surfactants are far superior to anionic monomeric surfactants in stabilizing curcumin at pH 9.2 and 13.0 where curcumin is partially or fully deprotonated to form the monoanionic or trianionic species (Cur^- or Cur^{3-}). An opposite charge of anionic curcumin with cationic surfactants favors the diffusion into micelles through electrostatic attraction.

Key Laboratory of Colloid and Interface Science, Beijing National Laboratory for Molecular Sciences (BNLMS), Institute of Chemistry, Chinese Academy of Sciences, Beijing 100190, China. E-mail: yilinwang@iccas.ac.cn; Fax: +86-10-82615802; Tel: +86-10-82615802

† Electronic supplementary information (ESI) available: UV-vis absorption spectra of Cur^{3-} in (a) 0 mM, (b) 0.060 mM, (c) 0.20 mM, (d) 0.60 mM, and (e) 2.00 mM over the course of 6 h at 1 h intervals. See DOI: 10.1039/c4sm00086b

Wang *et al.*[15] found that cationic gemini surfactants show higher efficacy in stabilizing Cur^{3-} at pH 13.0 than their monomeric counterparts. This is attributed to the fact that micelles formed by cationic gemini surfactants carry higher charge density than the monomeric counterparts, which leads to stronger electrostatic attraction with Cur^{3-}. In addition, the gemini surfactant concentration studied is much lower than its monomeric counterparts because the dimeric structure endows gemini surfactants with stronger self-assembly ability. In another work, the authors[16] further suggested that the spacer length of cationic gemini surfactants affects the chemical stability of Cur^{3-} in micelles by regulating the electrostatic attraction between surfactants and Cur^{3-}. Although the studies have constructed some relationship of the intermolecular interaction with the physicochemical properties of Cur^{3-} in surfactant micelles, the interaction mechanism of Cur^{3-} with surfactants and the effect of Cur^{3-} on the aggregation behavior of surfactants are still unclear. Wang *et al.*[17] spectroscopically investigated the interaction mechanism of neutral curcumin Cur^{0} with dodecyl trimethylammonium bromide DTAB in pH 5.0 sodium phosphate buffer and found that DTAB can aggregate into premicelles at concentrations prior to the micelle formation through dipole-charge and hydrophobic attractions. Compared with Cur^{0}, Cur^{3-} at pH 13.0 contains three negatively charged groups along its rigid conjugated structure. The anionic curcumin yields amphiphilic feature like surfactant organic additives salicylate and benzoate, which have been proved to effectively promote self-assembly of surfactants both in bulk solution and at air–water interface through strong electrostatic and hydrophobic interactions.[18,19]

Furthermore, the interaction of Cur^{3-} with cationic surfactants varies with the structure of surfactants. From molecular skeleton, cationic surfactants can be classified as classical monomeric surfactant and oligomeric surfactant with two or more identical or nearly identical monomeric amphiphilic fragments covalently connected by spacer groups.[20] As the number of monomeric amphiphilic fragments increases, cationic surfactants carry more positive charges and hydrophobic tails, and exhibit stronger self-assembly ability.[21–23] Therefore, hydrophobic and electrostatic interactions between cationic surfactants and Cur^{3-} probably increase with the degree of oligomerization, which will affect the aggregation behavior of surfactants. Systematically understanding the effect of the oligomeric degree of cationic surfactants on the interaction with Cur^{3-} will provide a guideline for selecting or designing even more suitable surfactants to improve the physicochemical properties of curcumin in micelle solution.

Thus, the central aim of the present work is to comparatively investigate the interaction of Cur^{3-} with a series of cationic surfactants with different numbers of monomeric amphiphilic fragments at pH 13.0 and the influence of Cur^{3-} on the aggregation behavior of these surfactants. The series of cationic surfactants include monomeric surfactant dodecyl trimethylammonium bromide (DTAB), gemini surfactant hexamethylene-1,6-bis(dodecyldimethylammonium bromide) (12–6–12) and trimeric surfactant tri(dodecyldimethylammonioacetoxy) diethyltriamine trichloride (DTAD), whose molecular structures and the molecular structure of curcumin are shown in Scheme 1. The surface tension and spectral methods have been employed to reveal the interaction mechanism and strength as well as the aggregate transitions in the mixed system. DTAD, 12–6–12 and DTAB exhibit similar interaction processes with Cur^{3-} in different surfactant concentration regions. The interaction strength between the cationic surfactants and Cur^{3-} is enhanced with increasing degree of oligomerization of the surfactants. However, either weak or strong interaction disfavors the solubility and stability of Cur^{3-} in surfactant micelles. Only the surfactant displaying moderate interaction with Cur^{3-} shows the best ability to improve the solubility and stability of Cur^{3-}. So 12–6–12 is the best one among these three surfactants. Furthermore, 12–6–12 was selected to further study the effect of the surfactant concentration on stabilizing Cur^{3-} and the binding model with Cur^{3-} was also investigated by isothermal titration calorimetry and ^{1}H NMR techniques.

Experimental section

Materials

Cationic gemini surfactant 12–6–12 was synthesized and purified according to the method of Zana *et al.*[24] Cationic trimeric surfactant DTAD was synthesized and purified as we reported previously.[25] Dodecyl trimethylammonium bromide DTAB (≥99%) and curcumin (≥98%) were purchased from Sigma-Aldrich Chemical Company and used without further purification. Sodium hydroxide (NaOH) (>96%) was purchased from Beijing Chemical Reagent Company. All measurements were performed at pH 13.0 adjusted by adding NaOH solution. The Milli-Q water (18.2 MΩ cm) was used in all experiments.

Surface tension

Surface tension measurement was carried out by the drop volume method. The end of the capillary used is flat surface and

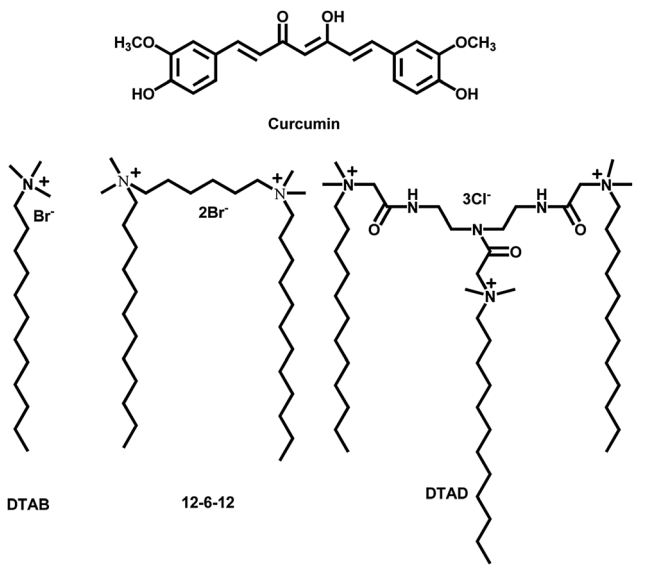

Scheme 1 The molecular structures of curcumin and the surfactants used.

the external radius (r) is 0.1535 cm. The volume (v) is adjusted by a Harkins and Brown correction factor which is a function of v/r^3. Each surface tension value (γ) was obtained by averaging at least five consistent measured values. The standard error of surface tension data is 1 mN m^{-1}. The measurement was conducted at 25.00 ± 0.05 °C using a thermostat.

Isothermal titration microcalorimetry (ITC)

Calorimetric measurements were conducted using a TAM 2277-201 microcalorimetric system (Thermometric AB, Järfälla, Sweden) with a stainless steel sample cell of 1 mL at 25.00 ± 0.01 °C. The cell was initially loaded with 700 μL of water or Cur^{3-} solution at pH 13.0. Each aliquot of 10 μL of concentrated 12–6–12 solution or concentrated 12–6–12–Cur^{3-} solution with a molar ratio of 3/2 was injected into the sample cell *via* a 500 μL Hamilton syringe controlled by a 612 Thermometric Lund pump. A series of injections were made until the desired range of concentrations had been covered. The solution in the sample cell was stirred at 50 rpm with a gold propeller. The observed enthalpy (ΔH_{obs}) was obtained by integration over the peak for each injection in the plot of heat flow P against time t and corrected by subtracting the enthalpy for the titration of water into water.

UV-visible absorption measurement

All UV-vis absorption measurements were performed with a fixed Cur^{3-} concentration of 20 μM. Absorbance measurements were performed using a UV 900 Hitachi spectrophotometer using a 1 cm path length quartz cuvette. The cuvette was initially loaded with 2 mL of 20 μM Cur^{3-}. The concentrated DTAB, 12–6–12 or DTAD solution with 20 μM Cur^{3-} was stepwise added into the aqueous Cur^{3-} solution and absorption spectra were recorded after each addition.

^{1}H NMR

^{1}H NMR measurements were carried out at 25 ± 2 °C on a Bruker AV400 FT-NMR spectrometer operating at 400.1 MHz. Deuteriumoxide (99.9%) was purchased from CIL Cambridge Isotope Laboratories and used to prepare the stock solutions of Cur^{3-} and 12–6–12 at pH 13.0. The center of the HDO signal (4.79 ppm) was used as the reference in the D_2O solutions. All the ^{1}H NMR experiments were recorded with a digital resolution of 0.04 Hz per data point.

Results and discussion

Interaction process of Cur^{3-} with DTAB, 12–6–12 and DTAD

In this section, the spectral variation of Cur^{3-} with surfactant concentration was applied to investigate the intermolecular interaction process of Cur^{3-} with DTAB, 12–6–12 and DTAD at pH 13.0. Before spectral measurements, the surface tension method was introduced to define the micellization of DTAB, 12–6–12 and DTAD under basic conditions in the presence and absence of Cur^{3-}. For the cases of the mixed solutions, the spectral and surface tension measurements were all carried out by titrating a small volume of concentrated surfactant solution with 20 μM Cur^{3-} into the Cur^{3-} solution of the same concentration at pH 13.0 so that the Cur^{3-} concentration remains constant during the entire titration process. The initial surfactant concentration is near or below the Cur^{3-} concentration 20 μM, and the final surfactant concentration is beyond the critical micelle concentrations of the three pure surfactants at neutral pH.[25–27] The adsorption spectra of Cur^{3-} at various surfactant concentrations are shown in Fig. 1(a1–a3). The maximum adsorption intensity I_{max} and the wavelength λ_{max} at I_{max} are presented in Fig. 1(b1–b3). The surface tension curves at pH 13.0 with and without Cur^{3-} are plotted against the surfactant concentration in Fig. 1(c1–c3). The top X axis of Fig. 1(b1–b3) represents the positive/negative charge ratio of the surfactant–Cur^{3-} mixture symbolized by +/−.

As shown in the surface tension curves in Fig. 1(c1–c3), the critical micelle concentration (CMC) values of DTAB, 12–6–12 and DTAD without Cur^{3-} are 7.00, 0.25 and 0.026 mM, respectively, corresponding to the break points of the curves. Comparing the surface tension curves of the surfactants in the presence of Cur^{3-} with the curves in the absence of Cur^{3-}, the critical micelle concentration of 12–6–12 with Cur^{3-} is significantly reduced and becomes 0.030 mM, whereas the critical micelle concentrations of DTAB and DTAD with Cur^{3-} almost have not been changed. The significant decrease of the critical micelle concentration of 12–6–12 must be caused by the interaction with Cur^{3-}. The critical micelle concentrations of these three surfactants with Cur^{3-} are designated as CMC_C, and the surface tension values of the surfactants with Cur^{3-} at CMC_C are lower than the surface tension values of the corresponding surfactants without Cur^{3-}. The lower surface tension values indicate that DTAB and DTAD also interact with Cur^{3-}. However, the interaction is insufficient to promote the micellization of DTAB and DTAD. Because the surface tension curves without Cur^{3-} do not show a minimum, the minimum in the curve of 12–6–12 or DTAD with Cur^{3-} also results from their interaction. The dashed lines in the figures are used to mark the positions of the CMC_C and the concentration C_M where the surface tension curves of the surfactants with Cur^{3-} initially merge into the surface tension curves of the surfactants without Cur^{3-}.

As seen, the adsorption spectra (Fig. 1(a1–a3)) of DTAB, 12–6–12 and DTAD bound Cur^{3-} show strong surfactant concentration dependence. As the surfactant concentration increases, a similar changing tendency of Cur^{3-} is observed for DTAB, 12–6–12 and DTAD, which indicates that Cur^{3-} undergoes a similar binding process with these three surfactants. First, the shoulder of Cur^{3-} at 350 nm gradually decreases with an increase of surfactant concentration and then disappears. The characteristic absorption at 350 nm comes from the π–π* excitation of short conjugated ferulic residues of Cur^{3-}.[28] Its decrease and absence with increasing surfactant concentration indicate that the surfactant binds on the active sites in the conjugated backbone of the ferulic units. From molecular structure, Cur^{3-} carries three negative charges along the conjugated structure with one in the middle enol group and two at either phenolic terminal of the ferulic units. Thus the electrostatic binding of the cationic headgroups of surfactants to the negative groups of the ferulic residues of Cur^{3-} may account for the decrease and absence of

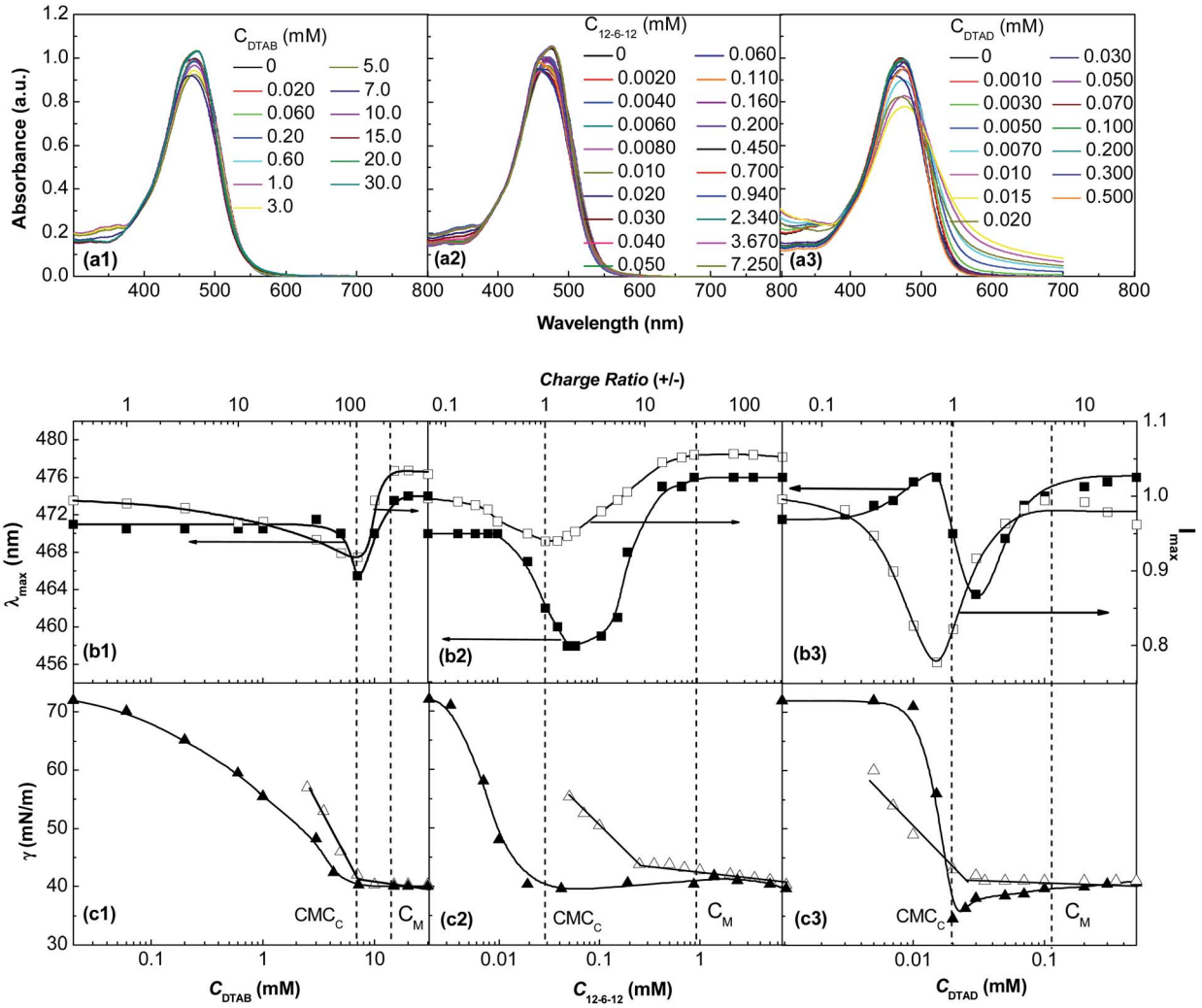

Fig. 1 (a1–a3) Absorption spectra of 20 μM Cur^{3-} with various DTAB, 12–6–12 and DTAD concentrations at pH 13.0. (b1–b3) Plots of I_{max} (□) and λ_{max} (■) *vs.* the surfactant concentration in the surfactant–Cur^{3-} mixture. For each plot, the left *Y* axis is λ_{max} and the right *Y* axis is I_{max}. (c1–c3) Variations of surface tension *vs.* the surfactant concentration at pH 13.0 in the presence (▲) and absence (Δ) of 20 μM Cur^{3-}.

the shoulder at 350 nm. Second, the intense absorption peak of Cur^{3-} around 470 nm shows complicated but regular change as the surfactant concentration increases (Fig. 1(b1–b3)). The characteristic absorption corresponds to the extended conjugated structure of Cur^{3-} itself.[28] Obviously the I_{max}–lg *C* and λ_{max}–lg *C* curves of Cur^{3-} with DTAB, 12–6–12 and DTAD exhibit transitions at CMC_C and C_M for all the three surfactants. This suggests that the interaction of the surfactants with Cur^{3-} can be divided into three regions. The surface tension and spectral variation in the different surfactant concentration regions will be discussed below.

Like normal surface tension curves of surfactants, the surface tension of DTAB or 12–6–12 in mixture with Cur^{3-} decreases as the surfactant concentration increases below CMC_C, while the surface tension of DTAD remains a constant of 72 mN m^{-1}, which is the same as that of water, and abruptly decreases until CMC_C. In the region below CMC_C, I_{max} of Cur^{3-} gradually decreases as the surfactant concentration increases whereas λ_{max} almost keeps a constant at low surfactant concentration and then abruptly decreases since the surfactant concentration is close to CMC_C. At the early stage of this region, λ_{max} of Cur^{3-} bound with DTAB or 12–6–12 remains constant at the value of the pure species (471 nm). Correspondingly, λ_{max} of Cur^{3-} bound with DTAD somewhat increases from 471 to 476 nm, then decreases as the surfactant concentration increases. At such dilute surfactant concentrations, cationic surfactant monomers tend to bind with Cur^{3-} through electrostatic and hydrophobic interactions, leading to ion association rather than micellization. Zsila *et al.*[28] have calculated the electron density distribution of curcumin and found that the middle enol group shows a maximum. Therefore, positively charged groups of added surfactants probably first attach to the central negatively charged groups of Cur^{3-}. As observed in protein–curcumin complexes,[1] this binding may disrupt the aromatic conjugated structure of Cur^{3-} by reducing the π–orbital overlap between two feruloyl chromophore units. Thus continuous addition of surfactants into Cur^{3-} solution in this region leads to the gradual decrease of I_{max} around 470 nm.

Additionally, sufficient cationic headgroups of surfactants will bind on the other negative charges of the ferulic units of Cur^{3-}. This binding leads to the consistent decrease of the absorption bands at both 350 and 470 nm. In a word, the electrostatic interaction between cationic surfactants and Cur^{3-} responds for the decrease of I_{max}. Compared with I_{max}, λ_{max} of Cur^{3-} below CMC_C is insensitive to a small amount of cationic surfactants, particularly to the monomeric cationic surfactant DTAB. Its invariable λ_{max} value at the early stage of this region implies that the electrostatic and hydrophobic interactions of DTAB with Cur^{3-} are the weakest among the three cationic surfactants. The abnormal increase of λ_{max} of Cur^{3-} bound with DTAD and the related high surface tension probably associate with the star-like trimeric structure of DTAD. DTAD carries three hydrophobic tails with separation due to the rigid pacer and intramolecular electrostatic repulsion among the three-charged headgroups. Considering the large number of positive charges and hydrophobic chains, Cur^{3-} prefers to bind on DTAD through strong electrostatic and hydrophobic interactions. As a consequence, the abundant alkyl tails of DTAD may form a hydrophobic microdomain for Cur^{3-}, which leads to the increase of λ_{max}. However, the extended structure and low concentration of bound DTAD are insufficient to alter the air–water interfacial properties and the resulting surface tension remains the same as that of water. The following decrease of λ_{max} of Cur^{3-} when the surfactant concentration approaches CMC_C suggests that the electrostatic interaction between them has been greatly enhanced. This enhanced electrostatic interaction may be understood from the pre-aggregation of the bound cationic surfactants driven by hydrophobic effects. When cationic surfactants exist as monomers in the dilute surfactant aqueous solution, hydration water of the surfactant molecule surface weakens the electrostatic interaction between the surfactants and Cur^{3-}. When the surfactant concentration is increased close to CMC_C, the hydrophobic effect is strong enough to promote the self-assembly of the bound alkyl chains of cationic surfactants accompanied by water release. The dehydration leads to stronger electrostatic interaction in the cationic surfactant–Cur^{3-} mixed system.

Above CMC_C, both I_{max} and λ_{max} of Cur^{3-} in turn increase with the increase of surfactant concentration and reach a large constant at C_M. The characteristic absorption at 350 nm starts to disappear above CMC_C. The reverse rise of I_{max} and λ_{max} of Cur^{3-} between CMC_C and C_M and the disappearance of the characteristic absorption at 350 nm suggest that the surfactant monomers bound with Cur^{3-} self-aggregate into micelles with Cur^{3-} trapped in. Thus, CMC_C represents the starting point where Cur^{3-} penetrates into the surfactant micelles. According to the surface tension curves, the CMC_C values of DTAB, 12–6–12 and DTAD with Cur^{3-} are about 7.00, 0.030 and 0.020 mM, respectively, where the positive/negative charge ratios of the surfactant to Cur^{3-} (+/−) are about 233, 1, 1. The required amounts of 12–6–12 and DTAD for the formation of the surfactant–Cur^{3-} mixed micelles are approximately 200-fold lower than DTAB. Such a lower dimeric or trimeric surfactant concentration for forming mixed micelles than the monomeric surfactant may be attributed to the following reasons. One reason is that pure 12–6–12 or DTAD exhibits higher self-aggregation ability than DTAB because of the synergistic effect of the dimeric or trimeric structure. This has been verified by many other groups and our group.[21–25] Generally, increasing the interaction of ionic surfactants with an oppositely charged additive can weaken the electrostatic repulsion between the headgroups and favor the micellization. So another probable reason is that the added Cur^{3-} and sodium hydroxide (NaOH) interact with the dimeric or trimeric surfactant more strongly than the monomeric surfactant. Herein, in order to adjust the solutions to pH 13.0, NaOH is needed to be added in, which has reduced the critical micelle concentration of DTAB by 50% and those of 12–6–12 and DTAD by one order of magnitude relative to the surfactants at neutral pH. The added Cur^{3-} further significantly decreases the critical micelle concentration of 12–6–12 but has almost no influence on the critical micelle concentration of DTAB and DTAD. The continuous decrease of the critical micelle concentration of 12–6–12 by adding Cur^{3-} must be caused by the strong intermolecular interaction between them. Above CMC_C, the surface tension of the DTAB–Cur^{3-} mixture remains a constant of 41 mN m^{-1} regardless of an increase in surfactant concentration, and finally overlaps with the surface tension of the surfactant without Cur^{3-} at C_M. Correspondingly, the surface tensions of the mixtures of Cur^{3-} with 12–6–12 and DTAD reach a minimum at CMC_C, beyond which the surface tensions of the 12–6–12–Cur^{3-} and DTAD–Cur^{3-} mixtures gradually increase as the surfactant concentration increases and then merge into the surface tension curves of the surfactants without Cur^{3-} at C_M. The minima in the surface tension curves of the 12–6–12–Cur^{3-} and DTAD–Cur^{3-} mixtures prove the stronger intermolecular interaction than the DTAB–Cur^{3-} mixture. The stronger interactions promote the binding and association of Cur^{3-} with 12–6–12 and DTAD and initiate the micellization of the mixtures at CMC_C, just corresponding to the equal charge point.

Beyond C_M, the binding of Cur^{3-} with the surfactants has reached saturation so that more added surfactants form free micelles like those without Cur^{3-}. Thus the surface tension curves with and without Cur^{3-} are merged with each other. And the I_{max} and λ_{max} values of Cur^{3-} bound with DTAB, 12–6–12 and DTAD reach a plateau, which indicates that all Cur^{3-} have been encapsulated in surfactant micelles. This means that C_M represents the initial point at which 20 μM Cur^{3-} is fully encapsulated in micelles. The C_M values of DTAB, 12–6–12 and DTAD are 15.0, 0.90 and 0.12 mM, as indicated in Fig. 1. The amount of surfactants required for full encapsulation of Cur^{3-} in micelles greatly decreases with the increase of the number of amphiphilic fragments of the surfactants. Cur^{3-} is likely to be located in the micellar palisade layer, resulting from a balance of electrostatic and hydrophobic interactions. The higher I_{max} and λ_{max} values of Cur^{3-} suggest that Cur^{3-} experiences more hydrophobic environments. The gemini surfactant micelles have stronger electrostatic and hydrophobic interactions with Cur^{3-} than the monomeric surfactant micelles, which facilitates Cur^{3-} to be trapped in a more hydrophobic microdomain. That is why the I_{max} and λ_{max} values of Cur^{3-} in the 12–6–12 micelles are larger than Cur^{3-} in the DTAB micelles. However,

the λ_{max} value of Cur^{3-} in the DTAD micelles is very close to that in 12–6–12 micelles, while the I_{max} value is almost the same as that of Cur^{3-} without any surfactants but lower than that in the 12–6–12 micelles. From the aspect of molecular structure, DTAD has the same amount of charges as Cur^{3-} but one more charge than 12–6–12. Thus the DTAD micelles should have stronger electrostatic interaction with Cur^{3-} than 12–6–12. The stronger interaction probably hinders Cur^{3-} bound with the headgroups of DTAD to penetrate into the DTAD micellar palisade layer as deeply as in the 12–6–12 micelles. In addition, the rigid spacer and strong electrostatic repulsion of the DTAD headgroups result that the palisade layer of DTAD near the headgroup area may be less hydrophobic than that of the 12–6–12 micelles. Therefore, I_{max} and λ_{max} of Cur^{3-} encapsulated in the DTAD micelles is close to or lower than in the 12–6–12 micelles.

In summary, the interaction of Cur^{3-} with these three surfactants experiences three different stages as the surfactant concentration increases and two transition points correspond to the critical micelle concentration of the surfactants with Cur^{3-} (CMC_C) and the initial point where the surface tension curves of the surfactants with and without Cur^{3-} overlap with each other (C_M). The three stages successively occur, including the binding of the surfactant monomers with Cur^{3-}, the formation of the surfactant–Cur^{3-} mixed micelles, and the formation of the free surfactant micelles. The basic Cur^{3-} solution decreases the critical micelle concentration of DTAB, 12–6–12 and DTAD. For the DTAB and DTAD cases, the added alkali is responsible for the decrease of the critical micelle concentration and the effect of Cur^{3-} can be neglected. For the 12–6–12 case, both alkali and Cur^{3-} contribute to the decrease of the critical micelle concentration. When the number of the amphiphilic fragments in surfactants is taken into account, the binding affinity towards Cur^{3-} increases with increasing degree of oligomerization, in the order of DTAB, 12–6–12 and DTAD. Because the loading ability of Cur^{3-} into micelles is driven by favorable hydrophobic and electrostatic interactions of Cur^{3-} with the surfactants, enhancing the oligomeric degree of surfactants may lead to an increase of the Cur^{3-} encapsulation and a decrease of the surfactant amount required. However, the very strong electrostatic interaction of Cur^{3-} with DTAD in the micelles makes Cur^{3-} locate near the micelle/water interface, which disfavors the stabilization of Cur^{3-}. In addition, very strong binding of Cur^{3-} with DTAD also makes the DTAD–Cur^{3-} mixture easily precipitate. That is to say, 12–6–12 is the best choice to encapsulate Cur^{3-}. In the following text, 12–6–12 is taken as a representative to investigate the concentration effect on the stabilization of Cur^{3-} and the interaction model of the surfactant with Cur^{3-}.

Effect of 12–6–12 concentration on stabilization of Cur^{3-}

Under basic conditions, curcumin will undergo a rapid alkaline hydrolysis which is initially fragmented into *trans*-6-(4′-hydroxy-3′-methoxyphenyl)-2,4-dioxo-5-hexanal and further decomposed into vanillin, ferulic acid and feruloyl methane.[10] Kee *et al.*[14] proved that the degradation products contribute negligibly to the entire absorption signal of Cur^{3-}. Thus, the degradation of Cur^{3-} can be expressed by a decrease of the characteristic absorption around 470 nm over time. Previous studies[13–16] on stabilizing Cur^{3-} emphasized that the surfactant concentrations used are at least twice the critical micelle concentration of the surfactant itself at neutral pH to ensure the formation of micelles for encapsulation. Actually, the added basic Cur^{3-} solution can effectively decrease the critical micelle concentration of surfactants as discussed above. The micelles for sequestrating Cur^{3-} from alkaline water already start to form far below the critical micellar concentration of surfactants without additives. Thus, a much less amount of surfactants is probably sufficient to stabilize Cur^{3-} against alkaline hydrolysis.

The UV-vis adsorption spectra measurements on degradation of 20 μM Cur^{3-} were carried out at various 12–6–12 concentrations. The minimum 12–6–12 concentration is 0.060 mM, which is higher than the critical micelle concentration of 12–6–12 with Cur^{3-} at pH 13.0 ($CMC_C = \sim 0.030$ mM). The maximum 12–6–12 concentration used is 2.00 mM, which is twice critical micelle concentration of 12–6–12 without Cur^{3-} at neutral pH. The spectra are shown in Fig. S1 of ESI.† The intense absorption peak of Cur^{3-} substantially loses its intensity with time for all the 12–6–12–Cur^{3-} mixed solutions but maintains the same position and shape. The residual Cur^{3-} (%) calculated from the absorption maxima is plotted against time (h) in Fig. 2.

At the first 3–4 hours, the residual Cur^{3-} linearly decreases with time. Then the decay of Cur^{3-} becomes slow. After 6 h incubation, about 23.0% of Cur^{3-} has been decomposed in water, while 16.0%, 4.6%, 5.9% and 7.5% of Cur^{3-} have been decomposed in 0.060, 0.20, 0.60 and 2.00 mM 12–6–12 solutions, respectively. Considering experimental errors, 0.20 mM 12–6–12 has shown the best effect in the suppression of Cur^{3-} degradation and higher 12–6–12 concentrations cannot improve the effect anymore. This concentration is ten times lower than those reported in the literature. The remarkable decrease of the 12–6–12 concentration for the stabilization of Cur^{3-} is attributed to the fact that the added basic Cur^{3-} solution effectively promotes the micellization of 12–6–12.

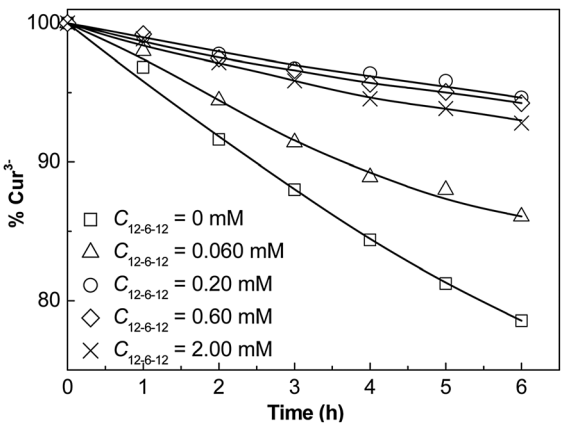

Fig. 2 Decay of 20 μM Cur^{3-} at the absorption maxima with various 12–6–12 concentrations at pH 13.0. The data are normalized to a value of 100 at zero time.

Interaction model between 12–6–12 and Cur^{3-} beyond CMC_C

On the basis of the above results, it can be concluded that 12–6–12 can effectively stabilize Cur^{3-} even at very low concentrations and it shows a high binding affinity to Cur^{3-} at pH 13.0. Thus, the positively charged groups of 12–6–12 may fully or partially bind on the negatively charged groups of Cur^{3-} to form the 12–6–12–Cur^{3-} complex. The bound or unbound state of surfactants varies with the surfactant concentration. Above C_M, the 12–6–12 concentration is very high relative to the Cur^{3-} concentration and the 12–6–12 molecules unbound with Cur^{3-} are dominated. So the aggregation behavior of the 12–6–12–Cur^{3-} mixture mainly shows the characteristics of 12–6–12 itself. However in the region of above CMC_C but below C_M, the 12–6–12 molecules unbound with Cur^{3-} become less and less with the decrease of the 12–6–12 concentration. The calculated positive/negative charge ratio of 12–6–12–Cur^{3-} is 1 at CMC_C and the minimum at CMC_C in the surface tension curve of the 12–6–12–Cur^{3-} mixture discloses the possibility of the formation of the 12–6–12–Cur^{3-} complex.

Fig. 3 shows the variations of surface tension and the observed enthalpy changes ΔH_{obs} against the logarithm of the 12–6–12 concentration at the fixed 12–6–12–Cur^{3-} molar ratio 3/2, *i.e.*, the positive/negative charge ratio +/− is 1. The breaking point in the surface tension curve corresponds to the critical micelle concentration of the 12–6–12–Cur^{3-} mixture (~0.024 mM), very close to the CMC_C at a fixed Cur^{3-} concentration derived from Fig. 2c2. The ITC experiment was also performed by following a similar titration process to the surface tension experiment, titrating concentrated 12–6–12–Cur^{3-} solution into the aqueous solution at pH 13.0. The dilution curve of the 12–6–12–Cur^{3-} mixture exhibits an approximate demicellization process with approximate S-shape profile and exothermic ΔH_{obs} values. The exothermic feature is present in the case of nonionic surfactants.[29,30] However, the ITC curve is deviated from the ITC curves of normal nonionic surfactants before the inflection point. This means that the dilution process of the 12–6–12–Cur^{3-} may involve a breaking process of the complexes beside the demicellization process. Thus, all the binding sites of Cur^{3-} are probably saturated by 12–6–12 to form a neutral complex and the resulting structure shows the characteristics of nonionic surfactants. Then the concentration of the inflection point in the ITC curve is consistent with the critical micelle concentration of the 12–6–12–Cur^{3-} complex derived from the surface tension curve. Similar to the oligomeric surfactants reported by Laschewsky and Zana,[20,21] the present 12–6–12–Cur^{3-} complex has a much lower critical micelle concentration than the monomeric and gemini counterparts. Previously, Huang *et al.*[31] found that the added sodium oligoarene sulfonates in DTAB can greatly decrease the critical micelle concentration. Our group[32,33] found the same phenomenon by adding an organic salt with multiple connecting sites into sodium dodecyl sulfate and proved the formation of oligomeric analogues through intermolecular interactions. Herein, Cur^{3-} carries three negative charges separately located on a rigid molecular structure and thus may bind with several oppositely charged molecules. Therefore, the 12–6–12–Cur^{3-} mixture at CMC_C may exhibit the characteristics of oligomeric surfactants.

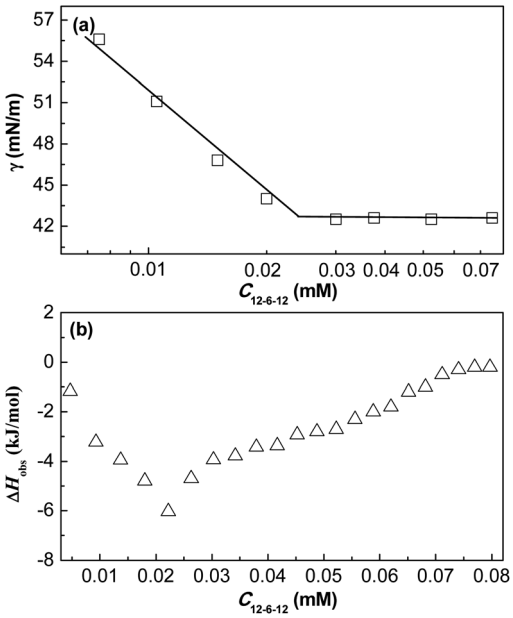

Fig. 3 Variation of surface tension (a) and the observed enthalpy changes (b) with the log of $C_{12-6-12}$ at the 12–6–12–Cur^{3-} molar ratio of 3/2 (+/− = 1).

To prove the above point, the ITC measurement was carried out by titrating concentrated 12–6–12 solution into 0.050 mM Cur^{3-} solution, and the observed enthalpy changes *versus* the 12–6–12–Cur^{3-} molar ratio are presented in Fig. 4. The ITC curve reflects the binding process of 12–6–12 with Cur^{3-} and is analyzed by standard Marquardt methods with an ITC package (supplied by Microcal Inc.) embedded in the Origin program to extract the binding parameters. The thermodynamic fitting curve to the ITC curve is shown by the red line. The derived binding stoichiometry n of 12–6–12 to Cur^{3-} is 2 and the binding constant K_b is $2.5 \times 10^4\ M^{-1}$. The n value represents the number of 12–6–12 bound on each Cur^{3-} where all the binding sites of 12–6–12 and Cur^{3-} are approximately thought to be identical. At pH 13.0, Cur^{3-} carries three negative charges without any other dipolar structure and thus it should have three binding sites with 12–6–12 molecules. Since each 12–6–12 carries two positive charges, it can bind with two charge sites of Cur^{3-}. That is to say, each Cur^{3-} molecule would need one and a half 12–6–12 molecules to saturate the binding sites and the resultant complex would be neutral. However, the n value obtained is 2. This means that about two 12–6–12 molecules are needed to saturate all the binding sites of each Cur^{3-} molecule. The extra one positive charge from the dimeric structure of 12–6–12 may be bound with another Cur^{3-} or just trapped in the mixed micelles.

The above discussion has confirmed the existence of the $(12\text{–}6\text{–}12)_2Cur^{3-}$ complex at CMC_C. To reveal the detailed intermolecular interaction, the ^1H NMR technique is employed and the ^1H NMR spectra of 12–6–12 at different concentrations in a 0.20 mM Cur^{3-} solution are shown in Fig. 5. For comparison purposes, the proton signals of 10.0 mM pure 12–6–12 solution without Cur^{3-} are also included. The proton signals of

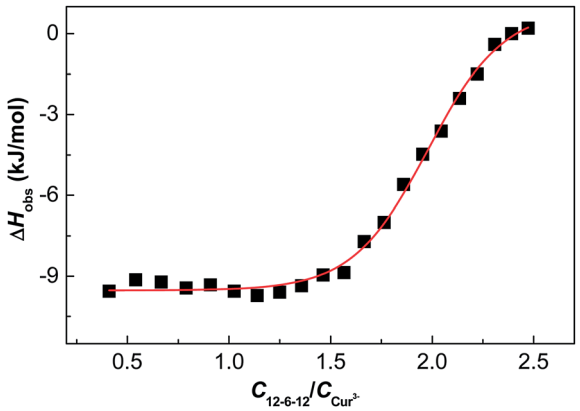

Fig. 4 The ITC experimental data of titrating 0.5 mM 12–6–12 to 0.050 mM Cur^{3-} and the thermodynamic fitting line. The binding number of 12–6–12 with Cur^{3-} is $n = 2$ and the binding constant is 2.5×10^4 M^{-1}.

Cur^{3-} are nearly merged into the baseline. Thus the ^1H NMR spectra of Cur^{3-} are not given.

Compared with the pure 12–6–12 (10.0 mM*), the addition of 0.20 mM Cur^{3-} causes almost no change for the chemical shifts of the 12–6–12 at higher 12–6–12 concentration because excess 12–6–12 molecules unbound with Cur^{3-} are a dominant component. In contrast, the peaks of the protons connecting or adjacent to the quaternary ammonium headgroups (H_e, $H_{e'}$, H_f, H_d, $H_{d'}$, H_c and $H_{c'}$) shift upfield whereas the peaks of the protons in the middle and end of hydrophobic chains (H_a and H_b) shift downfield. The reverse shifts of the H_d, $H_{d'}$, H_c and $H_{c'}$ peaks make them merge into the H_b peak at first and then split.

In the 12–6–12 concentration range studied, all the protons of 12–6–12 without Cur^{3-} have no obvious chemical shifts as the 12–6–12 concentration decreases. Thus, the variation of chemical shifts arising from the proton microenvironment change of 12–6–12 is induced by intermolecular interaction with Cur^{3-}. On one hand, the proximity of oxygen anions of Cur^{3-} to quaternary nitrogen cations of 12–6–12 reduces the tendency to withdraw electrons from the adjacent protons around the headgroups and the shielding effect results in upfield shifts. On the other hand, Cur^{3-} carries three oxygen anions along its conjugated structure and two of them on the end are directly linked on the benzene ring. Thus this terminal phenyl group of Cur^{3-} would stay near the headgroup of 12–6–12 through both electrostatic and hydrophobic interactions. This causes the protons adjacent to the headgroup of 12–6–12 to be located in the shielding region of the benzene ring of Cur^{3-}, which leads to the upshift. The two aspects synergistically affect the protons of 12–6–12 near the headgroup, leading to the marked upfield shifts. In contrast, the protons (H_a and H_b) in the alkyl chains of 12–6–12 exist in the shielding region of the benzene rings of Cur^{3-} and the shielding effect results in a downshift. As revealed by the above ITC result, 12–6–12 and Cur^{3-} can form the $(12\text{–}6\text{–}12)_2Cur^{3-}$ complex. The regular variation of all the proton peaks of 12–6–12 with the surfactant concentration indicates that the ratio of $(12\text{–}6\text{–}12)_2Cur^{3-}$ complex to free 12–6–12 increases with the decrease of the 12–6–12 concentration. When the 12–6–12 concentration decreases to 0.3 mM where the positive/negative charge ratio +/− is around 1, almost all the 12–6–12 and Cur^{3-} prefer to form the $(12\text{–}6\text{–}12)_2Cur^{3-}$ complex and the resultant proton signals are totally different from those of 12–6–12 without Cur^{3-}.

According to the above surface tension, ITC and ^1H NMR results, the $(12\text{–}6\text{–}12)_2Cur^{3-}$ complex is generated in the 12–6–12–Cur^{3-} mixed solution and the resulting structure shows the interface properties of oligomeric surfactants. The proposed schematic illustrations of the $(12\text{–}6\text{–}12)_2Cur^{3-}$ complex at air–water interface and in micelle are shown in Fig. 6. On the basis of the Chem3D simulation on Cur^{3-}, the distance between the oxygen anion in the middle and either oxygen anion at the end is estimated to be ~0.83 nm, which corresponds to the length of half Cur^{3-} molecule. The distance nearly matches with the spacer length between the two positive charges of 12–6–12 (~0.89 nm). This match enables the two headgroups of 12–6–12 to attach to the same Cur^{3-} molecule through electrostatic interaction assisted by hydrophobic interaction. One cationic charge of 12–6–12 is anchored to the central anionic group of Cur^{3-} and another cationic charge is attached to either terminal anionic group. Then the left unbound anionic group of Cur^{3-} binds to the second 12–6–12 molecule. Moreover the extra one positive charge of 12–6–12 will bind to another Cur^{3-}. As a consequence, both 12–6–12 and Cur^{3-} molecules play as links of the terminal unbound charge sites of the 12–6–12–Cur^{3-} complexes, forming a linear oligomeric surfactant analogue. The rigid aromatic backbone of Cur^{3-} may stay parallel to the spacer of 12–6–12 near the headgroup.

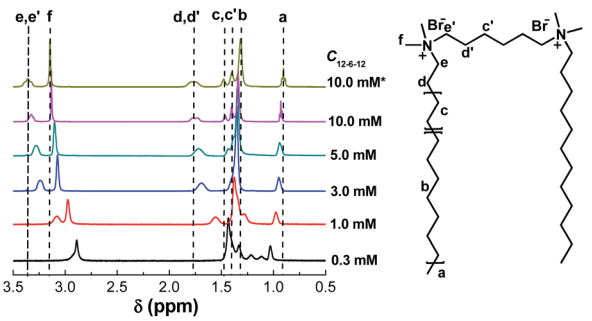

Fig. 5 ^1H NMR spectra and proton assignments of 12–6–12 at different concentrations (indicated in the plot) with a fixed Cur^{3-} concentration of 0.20 mM. *10.0 mM 12–6–12 without Cur^{3-}.

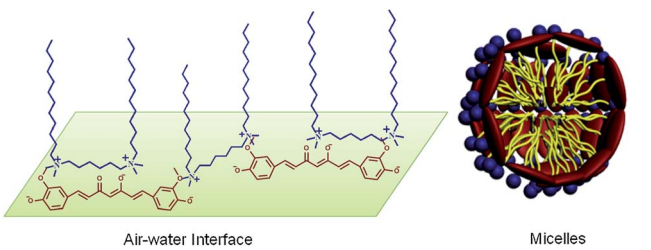

Fig. 6 Proposed schematic illustrations of the $(12\text{–}6\text{–}12)_2Cur^{3-}$ complex at air–water interface and in micelle. Br^- and Na^+ are not shown.

Conclusions

The interactions of Cur^{3-} with cationic monomeric surfactant DTAB, cationic gemini surfactant 12–6–12 and cationic trimeric surfactant DTAD have been investigated by surface tension, spectra and microcalorimetry methods. For all the three surfactant–Cur^{3-} mixtures, the surface tension and UV-vis adsorption spectra are surfactant concentration dependent. The added Cur^{3-} only decreases the critical micelle concentration of 12–6–12 instead of DTAB and DTAD. Below the critical micelle concentrations (CMC_C) of the surfactants in the presence of Cur^{3-}, the positive charges of the surfactants electrostatically bind with three negative charges of Cur^{3-} to cause ion associations. The formed surfactant–Cur^{3-} ion associations have lower surface tension values than the individual surfactants. Above CMC_C but below the concentration where the surface tensions of the surfactants with and without Cur^{3-} start to overlap (C_M), the bound and unbound surfactants aggregate into mixed micelles through hydrophobic interaction with Cur^{3-} trapped in the palisade layer. Above C_M, the excess unbound surfactants assemble into free micelles and all Cur^{3-} molecules are encapsulated in surfactant micelles. Apparently, increasing the oligomeric degree of cationic surfactants leads to stronger electrostatic and hydrophobic interactions with Cur^{3-} and a smaller amount of surfactants required for Cur^{3-} encapsulation. Compared with 12–6–12, both the weaker interaction of DTAB with Cur^{3-} and stronger interaction of DTAD with Cur^{3-} limit the stability or solubility of Cur^{3-} in surfactant micelles. Therefore, gemini surfactant 12–6–12 is the best choice to effectively suppress Cur^{3-} degradation at very low concentrations. Cationic gemini surfactant 12–6–12 and trianionic Cur^{3-} construct the $(12\text{–}6\text{–}12)_2Cur^{3-}$ complex with the structure feature of oligomeric surfactants owing to the bridging role of 12–6–12 or Cur^{3-}, which greatly improves the micellization ability of the surfactant and in turn greatly improves the encapsulation ability of 12–6–12 to Cur^{3-}. This work is helpful to understand the interaction of Cur^{3-} with cationic surfactants and helps to develop much more effective systems to stabilize Cur^{3-}. This understanding may be also helpful to design effective drug encapsulation systems.

Acknowledgements

We are grateful for financial support from Chinese Academy of Sciences and National Natural Science Foundation of China (grants 21025313.0, 21021003).

References

1 F. Zsila, Z. Bikádi and M. Simonyi, *Biochem. Biophys. Res. Commun.*, 2003, **301**, 776–782.
2 F. Zsila, Z. Bikádi and M. Simonyi, *Org. Biomol. Chem.*, 2004, **2**, 2902–2910.
3 A. J. Ruby, G. Kuttan, K. D. Babu, K. N. Rajasekharan and R. Kuttan, *Cancer Lett.*, 1995, **94**, 79–83.
4 B. B. Aggarwal, A. Kumar and A. C. Bharti, *Anticancer Res.*, 2003, **23**, 363–398.
5 M. X. Shi, Q. F. Cai, L. M. Yao, B. Y. Mao, Y. L. Ming and G. L. Ouyang, *Cell Biol. Int.*, 2006, **30**, 221–226.
6 R. C. Lantz, G. J. Chen, A. M. Solyom, S. D. Jolad and B. N. Timmermann, *Phytomedicine*, 2005, **12**, 445–452.
7 F. S. Yang, G. P. Lim, A. N. Begum, O. J. Ubeda and G. M. Cole, *J. Biol. Chem.*, 2005, **280**, 5892–5901.
8 N. Sreejayan and M. N. Rao, *Arzneim.-Forsch./Drug Res.*, 1996, **46**, 169–171.
9 M. Bernabé-Pineda, M. T. Ramírez-Silva, M. Romero-Romo, E. González-Vergara and A. Rojas-Hernandez, *Spectrochim. Acta, Part A*, 2004, **60**, 1091–1097.
10 Y. J. Wang, M. H. Pan, A. L. Cheng, L. I. Lin, Y. S. Ho and J. K. Lin, *J. Pharm. Biomed. Anal.*, 1997, **15**, 1867–1876.
11 H. H. Tønnesen, *Pharmazie*, 2002, **57**, 820–824.
12 C. F. Chignell, E. Morisbak and H. H. Tonnesen, *Photochem. Photobiol. Sci.*, 2005, **4**, 523–530.
13 Z. F. Wang, M. H. M. Leung, T. W. Kee and D. S. English, *Langmuir*, 2010, **26**, 5520–5526.
14 M. H. M. Leung, H. Colangelo and T. W. Kee, *Langmuir*, 2008, **24**, 5672–5675.
15 Z. Z. Wan, D. Ke, J. X. Hong, X. Y. Wang and W. G. Shen, *Colloids Surf., A*, 2012, **414**, 267–273.
16 D. Ke, Q. Q. Yang, M. L. Yang and X. Y. Wang, *Colloids Surf., A*, 2013, **436**, 80–86.
17 D. Ke, X. Y. Wang, Q. Q. Yang, Y. M. Niu and W. G. Shen, *Langmuir*, 2011, **27**, 14112–14117.
18 T. M. Clausen, P. K. Vinson, J. R. Minter and W. G. Miller, *J. Phys. Chem.*, 1992, **96**, 474–484.
19 D. F. Yu, X. Huang, M. L. Deng and Y. L. Wang, *J. Phys. Chem. B*, 2010, **114**, 14955–14964.
20 R. Zana, H. Levy, D. Papoutsi and G. Beinert, *Langmuir*, 1995, **11**, 3694–3698.
21 A. Laschewsky, L. Wattebled, M. Arotarena, J. Habib-Jiwan and R. H. Rakotoaly, *Langmuir*, 2005, **21**, 7170–7179.
22 M. In, V. Bec, O. Aguerre-Chariol and R. Zana, *Langmuir*, 2000, **16**, 141–148.
23 Y. B. Hou, Y. C. Han, M. L. Deng and Y. L. Wang, *Langmuir*, 2008, **26**, 28–33.
24 R. Zana, M. Benrraou and R. Rueff, *Langmuir*, 1991, **7**, 1072–1075.
25 C. X. Wu, Y. B. Hou, M. L. Deng and Y. L. Wang, *Langmuir*, 2010, **26**, 7922–7927.
26 R. Zana, *J. Colloid Interface Sci.*, 2002, **248**, 203–220.
27 P. Hansson, B. Joensson, C. Stroem and O. Soederman, *J. Phys. Chem. B*, 2000, **104**, 3496–3506.
28 F. Zsila, Z. Bikádi and M. Simonyi, *Tetrahedron: Asymmetry*, 2003, **14**, 2433–2444.
29 Y. J. Li, J. Reeve, Y. L. Wang, R. K. Thomas, J. B. Huang and H. K. Yan, *J. Phys. Chem. B*, 2005, **109**, 16070–16074.
30 S. Dai and K. C. Tam, *Colloids Surf., A*, 2003, **229**, 157–168.
31 L. X. Jiang, J. B. Huang, A. Bahramian, P. X. Li, R. K. Thomas and J. Penfold, *Langmuir*, 2012, **28**, 327–338.
32 D. F. Yu, M. Z. Tian, Y. X. Fan and Y. L. Wang, *J. Phys. Chem. B*, 2012, **116**, 6425–6430.
33 L. Y. Zhu, Y. C. Han, M. Z. Tian and Y. L. Wang, *Langmuir*, 2013, **29**, 12084–12092.

